A Vibronic Coupling Hamiltonian to Describe the Ultrafast Excited State Dynamics of a Cu(I)-Phenanthroline Complex

Gloria Capano[§ab], Thomas J. Penfold*[c], Ursula Röthlisberger[a], and Ivano Tavernelli[a]

[§]SCS-Metrohm Foundation Award for best oral presentation

Abstract: We present a model Hamiltonian to study the nonadiabatic dynamics of photoexcited $[Cu(dmp)_2]^+$, (dmp = 2,9-dimethyl-1,10-phenanthroline). The relevant normal modes, identified by the magnitude of the first order coupling constants, correspond closely to those observed experimentally. The potential energy surfaces (PES) and nonadiabatic couplings for these modes are computed and provide a first interpretation of the nonadiabatic relaxation mechanism. The Hamiltonian incorporates both the low lying singlet and triplet states, which will make it possible to follow the dynamics from the photoexcitation event to the initial stages of intersystem crossing.

Keywords: Cu(I)-phenanthroline complex · Multi-configuration time-dependent Hartree · Nonadiabatic · Vibronic coupling Hamiltonian · Time-dependent density functional theory

1. Introduction

Transition metal complexes play a central role as photocatalysts and as sensitizers in dye-sensitized solar cells.[1] Thus understanding their photodynamic properties is of fundamental as well as practical importance. Cu(I)-phenanthroline complexes are a class of systems that has recently received increasing attention. These compounds exhibit many properties similar to the popular ruthenium polypyridines, but have a lower coordination number of 4, which permits larger structural distortions in the excited state. While this offers greater flexibility to fine tune their photophysical properties, it also gives rise to strong structure-dependent energetics and susceptibility to solvent effects, which has so far hampered their development.[2]

Previous studies of the excited-state properties of Cu(I)-phenanthrolines have focused upon understanding their strongly solvent-dependent excited-state lifetimes which are significantly quenched in electron-donating solvents.[3] This has been attributed to the complexation of a solvent molecule to the metal center in the excited state,[3c] which becomes possible due to the pseudo Jahn-Teller (PJT) distortion of the ligands, exposing the copper ion to the solvent. However, using time-resolved X-ray absorption spectroscopy,[4] combined with first-principles molecular dynamics simulations in explicit solvent, we have recently shown that this is not the case.[5] Instead, the solvent interaction is transient and arises from a particular solvent structure that is also present in the electronic ground state. To reduce the influence of the surrounding solvent and to prolong the excited-state lifetime, it is important that structural modifications of the phenanthroline-derived ligands are performed in such a way that they are able to disrupt the structure of the first solvation shell.[6]

Importantly, these modifications not only affect the interaction with the solvent, but also the femtosecond (fs) dynamics that follow photoexcitation, characterized by couplings between multiple excited states leading to strong nonadiabatic effects. Ultrafast absorption and emission studies used to probe these photodynamics have focused upon the prototypical Cu(I)-phenanthroline complex, $[Cu(dmp)_2]^+$.[7] Tahara and co-workers[7a] concluded that upon photoexcitation, decay of the initially populated state occurs with a time constant of ≈45 fs. This is followed by two other processes of ≈660 fs and ≈7.4 ps, which were assigned to a PJT distortion (ligand flattening) and intersystem crossing, respectively. In a later study,[7b] they also probed the time-evolution in the lowest singlet Metal-Ligand Charge Transfer (MLCT) state, using the observed dynamics to predict the most important normal modes activated during the excited-state dynamics. Interestingly, they also reported that the S_1 state exhibits a small energetic barrier leading to the PJT distortion. However, such a barrier is at odds with the spontaneous structural instability usually associated with JT type effects.

For a full understanding of the excited-state dynamics of such complexes, simulations provide an important tool. In this contribution we present a Vibronic Coupling Hamiltonian suitable for use in quantum nuclear dynamics to study the excited-state properties of $[Cu(dmp)_2]^+$. We identify the normal modes which are most relevant and discuss the calculated PES along these modes in relation to the excited-state dynamics. The Hamiltonian incorporates both the low lying singlet and triplet states, which makes it possible to probe the entire dynamics during the first picosecond (ps) after photoexcitation.

2. Theory

To describe the nonadiabatic dynamics of $[Cu(dmp)_2]^+$ we use the Vibronic Coupling Hamiltonian, described in ref. [8].

*Correspondence: Dr. T. J. Penfold[c]
E-mail: thomas.penfold@psi.ch
[a]Laboratory of Computational Chemistry and Biochemistry
Ecole Polytechnique Fédérale de Lausanne
CH-1015 Lausanne
[b]Laboratory of Ultrafast Spectroscopy
Ecole Polytechnique Fédérale de Lausanne
CH-1015 Lausanne
[c]SwissFEL
Paul Scherrer Institute
CH-5232 Villigen

Briefly, an N state Hamiltonian, is expressed using an N*x*N matrix and expanded as a Taylor series around the Franck-Condon (FC) point Q_0:

$$\hat{\mathbf{H}} = \hat{\mathbf{H}}_\mathbf{0} + \hat{\mathbf{W}}^{(\mathbf{0})} + \hat{\mathbf{W}}^{(\mathbf{1})} + \hat{\mathbf{W}}^{(\mathbf{2})} \quad (1)$$

The first term includes the kinetic energy operator and a harmonic term representing the ground state Hamiltonian. $\hat{W}^{(0)}$ is the zeroth order diagonal coupling matrix which contains the vertical excited state energies at the FC geometry. The third term, $\hat{W}^{(1)}$, contains the linear coupling elements expressed as:

$$\hat{W}^{(1)}_{nn} = \langle\phi_n|\frac{\partial \hat{H}_{el}}{\partial Q_i}|\phi_n\rangle Q_i \quad (2)$$

and

$$\hat{W}^{(1)}_{nn'} = \langle\phi_n|\frac{\partial \hat{H}_{el}}{\partial Q_i}|\phi_{n'}\rangle Q_i \quad (3)$$

where ϕ_n are the electronic wavefunctions. The quantities within the Dirac brackets are the on- (Eqn. (2)) and off-diagonal (Eqn. (3)) coupling constants, usually represented by $\kappa_i(n)$ and $\lambda_i(n,n')$, respectively. The on-diagonal terms are related to the derivative of the adiabatic PES with respect to the coordinates and represent the forces acting on the diabatic surface. The off-diagonal terms are the nonadiabatic couplings.

The second order ($\hat{W}^{(2)}$) nonadiabatic coupling terms are generally small and usually neglected, however the on-diagonal terms can play an important role and are expressed:

$$W^{(2)}_n = \frac{1}{2}\sum_{i,j}\langle\phi_n|\frac{\partial^2 \hat{H}_{el}}{\partial Q_i \partial Q_j}|\phi_n\rangle Q_i Q_j \quad (4)$$

In this case, the quantity within the Dirac brackets is usually referred to as $\gamma_{i,j}(n)$. When $Q_i = Q_j$ the coupling occurs within a nuclear degree of freedom (DOF) and causes a change of frequency of the excited state potential. For $Q_i \neq Q_j$ (bilinear), coupling occurs between two nuclear DOFs and is responsible for intramolecular vibrational redistribution.

In the Hamiltonian in Eqn. (1), the number of expansion coefficients (*i.e.* κ, λ and γ) can quickly become very large as the number of DOFs increases. To reduce computational cost, symmetry constraints may be used. For the linear terms, the expansion coefficients are non-zero only when the product of the irreducible representation of the electronic states and of the vibrational DOF is totally symmetric. For the D_2 point group relevant for the copper phenanthroline complexes considered here we can write,

$$\Gamma_n \times \Gamma_{Q_i} \times \Gamma_{n'} \supset \Gamma_A \quad (5)$$

where Γ_n and $\Gamma_{n'}$ are the irreducible representations of the states *n* and *n'* and Γ_{Qi} is the irreducible representation of normal mode Q_i.[8]

The expansion coefficients expressed in Eqns (2)–(4) have been obtained by performing a fit to quantum chemistry points calculated at nuclear geometries along the relevant normal modes, using DFT. Couplings between the vibrational DOFs were calculated using diagonal cuts through pairs of normal modes. The ground and excited state energies were calculated using DFT/TDDFT as implemented in Gaussian09[9] within the approximation of the B3LYP functional.[10] For all calculations a TZVP basis set was used for the copper atom and an aug-SVP basis set for N, C and H. The fit of the PES was performed using the VCHAM program, distributed with the Heidelberg MCTDH package.[11]

3. Results and Discussion

$[Cu(dmp)_2]^+$ has 57 atoms and therefore 165 normal modes. Consequently, calculating the full PES is unrealistic. To reduce the computational effort we use a model Hamiltonian that includes only the most important vibrational DOFs for the ultrafast dynamics under study. In fact, while this approximated Hamiltonian will be unable to capture longer time effects, such as vibrational cooling (≈10 ps[7d]), the approximations made will have little influence on the dynamics during the first ps.[7d]

3.1 *Zeroth-order Expansion Coefficients*

The zeroth-order coefficients ($\hat{W}^{(0)}$) are reported in Table 1. All of these states are composed of an excitation from a metal d-orbital to a ligand π^* orbital (Fig. 1) and are therefore MLCT states.[12]

The lowest four triplet states are all below the S_1 state and all lie in a close energy range of ≈0.1 eV. The lowest two singlet states (S_1 and S_2) have excitation energies of 2.44 and 2.51 eV, respectively, at the ground state optimized geometry. In previous simulations which constrained the structure to a D_{2d} symmetry,[7d,12] these states are degenerate. However, no such constraints were used in this study and we

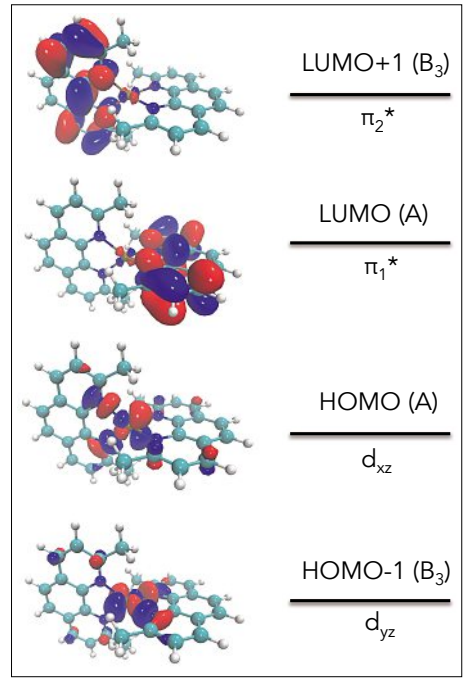

Fig. 1. Molecular orbital diagram and characteristics of the HOMO-1, HOMO, LUMO, and LUMO+1 orbitals involved in the low lying excited states of $[Cu(dmp)_2]^+$. Contour levels drawn at 0.02 a.u.

Table 1. Excitation energies (eV) and oscillator strength of the singlet and triplet states of $[Cu(dmp)_2]^+$ at the ground-state equilibrium geometry calculated using TD-DFT with the B3LYP functional.

State	Symmetry	Energy [eV]	Oscillator Strength	Description[a]
S_1	$^1B_3$	2.44	0.0006	$d_{yz}\rightarrow\pi_1^*$, $d_{xz}\rightarrow\pi_2^*$
S_2	^1A	2.51	0.0000	$d_{yz}\rightarrow\pi_2^*$, $d_{xz}\rightarrow\pi_1^*$
S_3	$^1B_3$	2.70	0.1608	$d_{xz}\rightarrow\pi_1^*$, $d_{xz}\rightarrow\pi_2^*$
T_1	^3A	2.27	-	$d_{yz}\rightarrow\pi_2^*$
T_2	^3A	2.31	-	$d_{yz}\rightarrow\pi_1^*$
T_3	$^3B_3$	2.33	-	$d_{xz}\rightarrow\pi_1^*$
T_4	$^3B_3$	2.37	-	$d_{xz}\rightarrow\pi_2^*$

[a]See Fig. 1 for a representation of the orbitals. The dominant characters of the electronic transitions are indicated.

find that the lowest energy structure has D_2 symmetry, giving rise to a small but sizable splitting of these states. The S_3 state, whose transition from the ground state is dipole-allowed, has an energy of 2.70 eV and closely corresponds to the maximum observed in the experimental absorption spectra of $[Cu(dmp)_2]^+$, 2.73 eV.[7c]

3.2 *First-order Expansion Coefficients*

The first-order terms arise from coupling of the electronic states to a specific nuclear DOF (Eqns (2) and (3)). Based on the magnitude of the linear coupling constants we have identified eight normal modes that are likely to be dominant in the initial photoexcited dynamics (Table 2). Although this clearly represents a significant reduction in the dimensionality of the investigated configuration space, the modes included closely correspond to those identified in the emission study of ref. [7b]. Cuts through the PESs along some of the most important modes (ν_8, ν_{19}, ν_{21} and ν_{25}) are depicted in Fig. 2.

Owing to symmetry, only modes ν_8 and ν_{25} can yield non-zero on-diagonal linear coupling coefficients (κ). Indeed, both of these modes exhibit excited-state minima that are shifted with respect to the ground-state equilibrium position (an effect of on-diagonal linear coupling). For ν_8, this shift reflects a strengthening of the Cu–N bonds in the excited state, which is supported by experimental observations[6] and is due to the π back-donation character of the ligands and the enhanced electrostatic interaction between metal and ligands following the charge transfer excitation.

Along ν_{25}, the S_1 and S_2 states also exhibit a shortening of the Cu–N bonds. In contrast the triplet states exhibit a profile more reminiscent of a PJT distortion with an asymmetric double minimum profile. This behavior is due to linear off-diagonal coupling between the T_1/T_2 and T_3/T_4 states (Table 3).

The modes ν_{19} and ν_{21} have b_3 symmetry and correspond to a flattening motion of the two ligands and to an off center movement of the Cu atom, respectively. The on-diagonal linear coupling coefficients (κ) are always zero by symmetry, however the off-diagonal expansion coefficients (λ) can be non-zero between states S_3/S_2 and S_2/S_1. As shown in Table 3 these modes strongly couple the S_1 and S_2 surfaces and are responsible for the PJT effects in $[Cu(dmp)_2]^+$. This effect is strongest in ν_{21} where both the lowest singlet and triplet states are strongly characterized by double minima profiles located symmetrically with respect to the ground state equilibrium position, which arises from the aforementioned coupling. The effect is weaker for ν_{19}. Finally, as shown in Table

Table 2. Symmetry and frequency (cm^{-1}) of the selected normal modes. The normal modes were calculated using DFT within the approximation of the B3LYP functional. The experimental values are taken from ref. [6a].

Mode	Symmetry	Theory [cm^{-1}]	Expt. [cm^{-1}]	Description
ν_8	a	99.16	125	Breathing
ν_{19}	b_3	193.61	191	Rocking
ν_{21}	b_3	247.61	240	Rocking
ν_{25}	a	270.85	290	Twist
ν_{31}	b_3	420.77	438	Bending
ν_{41}	b_3	502.65	–	Bending
ν_{55}	b_3	704.75	704	Rocking
ν_{58}	b_3	790.76	–	Rocking

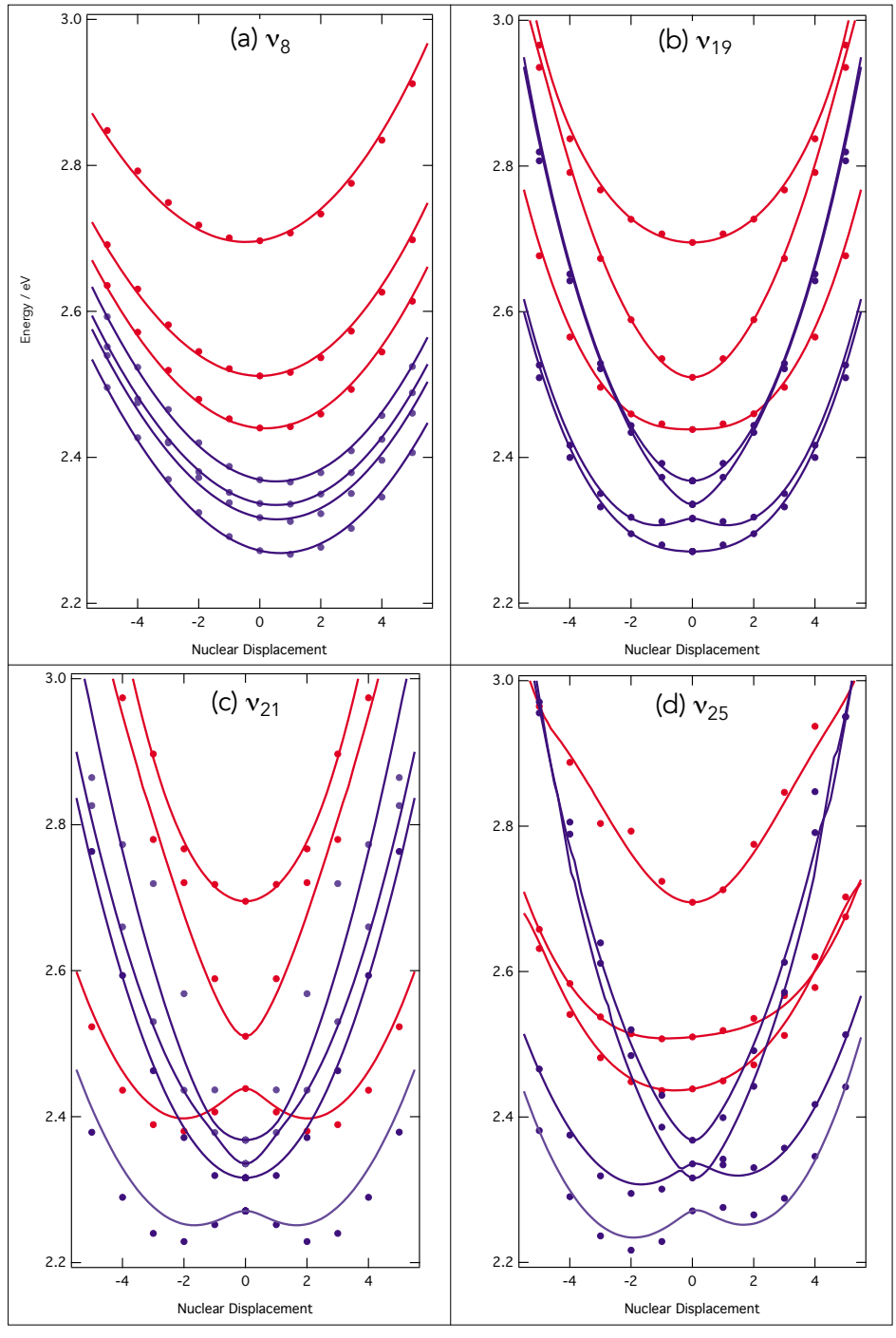

Fig. 2. Cuts through the PES along a) ν_8, b) ν_{19}, c) ν_{21} and d) ν_{25}. The dots are results from the quantum chemistry calculations for the singlet (red) and triplet (blue) states. The lines correspond to their fit from which the expansion coefficients are determined.

Table 3. On-diagonal (κ) and off-diagonal (λ) linear coupling constants in eV for the selected vibrational modes of $[Cu(dmp)_2]^+$.

	ν_{19}	ν_{21}	ν_{25}	ν_{31}	ν_{41}	ν_{55}	ν_{58}
κ_S	–	–	0.0053	–	–	–	–
κ_{S2}	–	–	0.0070	–	–	–	–
κ_{S3}	–	–	–0.0031	–	–	–	–
$\lambda_{S1\text{-}S2}$	0.0027	0.0695	–	0.0463	0.0156	0.0218	0.0417
$\lambda_{S1\text{-}S3}$	–	–	0.0275	–	–	–	–
$\lambda_{S2\text{-}S3}$	0.0520	0.0178	-	0.0145	0.0077	–	–0.0020
$\lambda_{T1\text{-}T2}$	–	–	0.0491	–	–	–	–
$\lambda_{T1\text{-}T3}$	–0.0033	0.0512	–	0.0243	0.0860	0.0136	0.0136
$\lambda_{T1\text{-}T4}$	0.0267	0.0137	–	0.0243	0.0073	0.0126	0.0310
$\lambda_{T2\text{-}T3}$	–0.0296	0.0051	–	0.0323	0.0115	0.0107	0.0342
$\lambda_{T2\text{-}T4}$	0.0011	–	–	–	0.0068	0.0137	0.0042
$\lambda_{T3\text{-}T4}$	–	–	0.0441	–	–	–	–

3 we also find an off-diagonal expansion coefficient (λ) along the ν_{25} coupling the S_3 and S_1 states. This offers the possibility for the wavepacket to relax directly from the initially populated state into the lowest singlet state, however given the large energy separation and the strong coupling between the S_1 and S_2 states, this pathway will likely provide only these a minor contribution to the overall dynamics.

3.3 *Second-order Expansion Coefficients*

All of the modes considered in this work require on-diagonal second-order coupling terms (Table 4), which account for a change of frequency of the excited state potentials compared to the ground state. However we find that they are all relatively small, meaning that their effect is expected to be negligible.

In addition, small bilinear terms were also fitted between each pair of modes. These terms, which are responsible for redistribution of vibrational energy formed during the electronic relaxation, were found to be smaller than <0.005 eV. Although these terms will have an important role for long time dynamics associated with vibrational cooling, such effects are beyond the scope of our investigation since their effect on the short time (<1 ps) dynamics is expected to be small.

4. Conclusions and Outlook

Using TDDFT, we have calculated a model Hamiltonian based upon the Vibronic Coupling *ansatz*. Our calculated PES show that at the equilibrium geometry, which possesses D_2 symmetry, the optically bright state is the S_3 MLCT state. Importantly, the two excited states which lie below S_3 are very close in energy, and are strongly coupled. This means that the rate of internal conversion into the S_1 PJT minimum, and ultimately the triplet states, will be strongly determined by the rate of nonadiabatic relaxation between the S_3 and S_2 states, which are weakly coupled and are separated by a larger energy gap. In addition, contrary to previous observations[7a] the present PESs calculated in this work do not exhibit a barrier leading to the PJT distortion in the excited state. The Hamiltonian derived in this work can be used, in conjunction with nuclear quantum dynamics simulations, to shed new insights into the ultrafast excited state dynamics of $[Cu(dmp)_2]^+$.

Table 4. On-diagonal (λ) second-order coupling constants in eV for the selected vibrational modes of $[Cu(dmp)_2]^+$.

	ν_8	ν_{19}	ν_{21}	ν_{25}	ν_{31}	ν_{41}	ν_{55}	ν_{58}
γ_{S1}	0.0027	0.0010	0.0035	–0.0183	0.0124	0.0020	0.0024	0.0034
γ_{S2}	0.0015	0.0004	0.0032	–0.0069	–0.0011	0.0027	–	0.0035
γ_{S3}	–0.0011	–0.0029	0.0054	0.0067	–0.0029	0.0017	0.0022	0.0029
γ_{T1}	–	–	–0.0009	–0.0099	0.0016	0.0020	0.0020	0.0021
γ_{T2}	–	–0.0041	0.0038	–0.0035	0.0022	0.0021	0.0016	0.0047
γ_{T3}	–	0.0007	–0.0006	–0.0079	0.0027	0.0022	0.0021	0.0018
γ_{T4}	–	0.0001	0.0051	–0.0036	0.0051	0.0020	0.0016	0.0052

Acknowledgements

We thank the Swiss National Science Foundation Grant 200021-137717 and the NCCR MUST interdisciplinary research program.

Received: January 17, 2014

[1] a) B. Kumar, M. Llorente, J. Froehlich, T. Dang, A. Sathrum, C. P. Kubiak, *Ann. Rev. Phys. Chem.* **2012**, *63*, 541; b) B. O'Regan, M. Grätzel, *Nature* **1991**, *353*, 24.
[2] N. Armaroli, *Chem. Soc. Rev.* **2001**, *30*, 113.
[3] a) D. R. McMillin, J. R. Kirchhoff, K. V. Goodwin, *Coord. Chem. Rev.* **1985**, *64*, 83; b) C. T. Cunningham, K. L. H. Cunningham, J. F. Michalec, D. R. McMillin, *Inorg. Chem.* **1999**, *38*, 4388; c) L. X. Chen, G. Shaw, I. Novozhilova, T. Liu, G. Jennings, K. Attenkofer, G. Meyer, P. Coppens, *J. Am. Chem. Soc.* **2003**, *125*, 7022.
[4] T. J. Penfold, C. J. Milne, M. Chergui, *Adv. Chem. Phys.* **2013**, *153*, 1.
[5] T. J. Penfold, S. Karlsson, G. Capano, F. A. Lima, J. Rittmann, M. Reinhard, H. Rittmann-Frank, O. Bräm, E. Baranoff, R. Abela, I. Tavernelli, U. Rothlisberger, C. J. Milne, M. Chergui, *J. Phys. Chem. A* **2013**, *117*, 4591.
[6] C. E. McCusker, F. N. Castellano, *Inorg. Chem.* **2013**, *52*, 8114.
[7] a) M. Iwamura, S. Takeuchi, T. Tahara, *J. Am. Chem. Soc.* **2007**, *129*, 5248; b) M. Iwamura, H. Watanabe, K. Ishii, S. Takeuchi, T. Tahara, *J. Am. Chem. Soc.* **2011**, *133*, 7728; c) Z. Siddique, Y. Yamamoto, T. Ohno, K. Nozaki, *Inorg. Chem.* **2003**, *42*, 6366; d) G. Shaw, C. Grant, H. Shirota, E. Castner, G. Meyer, L.X. Chen, *J. Am. Chem. Soc.* **2007**, *129*, 2147.
[8] a) C. Cattarius, G. A. Worth, H.-D. Meyer, *J. Chem. Phys.* **2001**, *131*, 2088; b) T. J. Penfold, G. A. Worth, *J. Chem. Phys.* **2009**, *131*, 064303; c) T. J. Penfold, R. Spesyvtsev, O. M. Kirkby, R. S. Minns, D. S. N. Parker, H. H. Fielding, G. A. Worth, *J. Chem. Phys.* **2012**, *137*, 204310.
[9] M. J. Frisch, G. W. Trucks, H. B. Schlegel, G. E. Scuseria, M. Robb, J. R. Cheeseman, G. Scalmani, V. Barone, B. Mennucci, G. A. Petersson, H. Nakatsuji, M. Caricato, X. Li, H. P. Hratchian, A. F. Izmaylov, J. Bloino, G. Zheng, J. L. Sonnenberg, M. Hada, M. Ehara, K. Toyota, R. Fukuda, J. Hasegawa, M. Ishida, T. Nakajima, Y. Honda, O. Kitao, H. Nakai, T. Vreven, J. A. A. Montgomery, J. E. Peralta, F. Ogliaro, M. Bearpark, J. J. Heyd, E. Brothers, K. N. Kudin, V. N. Staroverov, R. Kobayashi, J. Normand, K. Raghavachari, A. Rendell, J. C. Burant, S. S. Iyengar, J. Tomasi, M. Cossi, N. Rega, J. M. Millam, M. Klene, J. E. Knox, J. B. Cross, V. Bakken, C. Adamo, J. Jaramillo, R. Gomperts, R. E. Stratmann, O. Yazyev, A. J. Austin, R. Cammi, C. Pomelli, J. W. Ochterski, R. L. Martin, K. Morokuma, V. G Zakrzewski, G. A. Voth, P. Salvador, J. J Dannenberg, S. Dapprich, A. D. Daniels, V. Farkas, J. B Foresman, J. V. Ortiz, J. Cioslowski, D. J. Fox, Gaussian Inc., Wallingford, CT, **2009**.
[10] a) A. D. Becke, *J. Chem. Phys.* **1993**, *98*, 5648; b) C. Lee, W. Yang, R. G. Parr, *Phys. Rev. B* **1988**, *37*, 785; c) S. H. Vosko, L. Wilk, M. Nusair, *Can. J. Phys.* **1980**, *58*, 1200; d) P. J. Stephens, F. J. Devlin, C. F. Chabalowski, M. J. Frisch, *J. Phys. Chem.* **1994**, *98* 11623.
[11] M. Beck, A. Jackle, G. A. Worth, H.-D. Meyer, *Phys. Rep.* **2000**, *324*, 1.
[12] M. Zgierski, *J. Chem. Phys.* **2003**, *118*, 4045.